Monitoring Delamination of Plasma-Sprayed Thermal Barrier Coatings by Reflectance-Enhanced Luminescence

Jeffrey I. Eldridge and Timothy J. Bencic

NASA Glenn Research Center
Cleveland, OH

Abstract

Highly scattering plasma-sprayed thermal barrier coatings (TBCs) present a challenge for optical diagnostic methods to monitor TBC delamination because scattering attenuates light transmitted through the TBC and usually degrades contrast between attached and delaminated regions of the TBC. This paper presents a new approach where reflectance-enhanced luminescence from a luminescent sublayer incorporated along the bottom of the TBC is used to identify regions of TBC delamination. Because of the higher survival rate of luminescence reflecting off the back surface of a delaminated TBC, the strong scattering exhibited by plasma-sprayed TBCs actually accentuates contrast between attached and delaminated regions by making it more likely that multiple reflections of luminescence off the back surface occur before exiting the top surface of the TBC. A freestanding coating containing sections designed to model an attached or delaminated TBC was prepared by depositing a luminescent Eu-doped or Er-doped yttria-stabilized zirconia (YSZ) luminescent layer below a plasma-sprayed undoped YSZ layer and utilizing a NiCr backing layer to represent an attached substrate. For specimens with a Eu-doped YSZ luminescent sublayer, luminescence intensity maps showed excellent contrast between unbacked and NiCr-backed sections even at a plasma-sprayed overlayer thickness of 300 μm. Discernable contrast between unbacked and NiCr-backed sections was not observed for specimens with a Er-doped YSZ luminescent sublayer because luminescence from Er impurities in the undoped YSZ layer overwhelmed luminescence originating form the Er-doped YSZ sublayer.

1. Introduction

While thermal barrier coatings (TBCs), most often composed of yttria-stabilized zirconia (YSZ), provide beneficial thermal protection to turbine engine components,[1] the risk of TBC spallation necessitates scheduled TBC replacement that is not currently based on an informed assessment of TBC damage. Because the spallation of plasma-sprayed TBCs typically proceeds by the gradual growth and networking of subsurface delamination cracks,[2] nondestructive diagnostics that can assess hidden subsurface delamination progression could be utilized to prompt TBC replacement well before the level of TBC damage compromises engine performance or safety. Optical methods, such as piezospectroscopy [3] and optical elastic scattering,[4] can be used to probe subsurface damage in translucent TBCs. However, these methods are much more successful for probing through the thickness of electron-beam physical vapor deposited (EB-PVD) TBCs than for probing through the much more highly scattering plasma-sprayed TBCs. [5] While mid-infrared (MIR) reflectance [6-7] was shown to detect the increased reflectance at 4 μm wavelength that accompanies subsurface crack propagation in plasma-sprayed TBCs, the relative increase in overall reflectance associated with TBC delamination was modest due to the presence of strong background scattering from the pre-existing porosity and cracks present throughout the TBC. This background volume scattering cannot be distinguished from scattering by subsurface delamination cracks, making delamination monitoring difficult for thicker plasma-sprayed TBCs. This paper presents an alternative approach that monitors luminescence intensity produced by a rare-earth doped YSZ luminescent sublayer incorporated along the base of the TBC. In this approach, increased luminescence intensity is used to identify the location and severity of TBC delamination progression. The increased luminescence intensity associated with TBC delamination is due to increased reflectance of both the excitation and emission wavelengths by the subsurface delamination cracks. Because all observed luminescence originates from the luminescent sublayer, there is no competing background signal originating through the remaining

TBC volume as is the case with MIR reflectance. Using a simple freestanding coating design that mimics TBC delamination, this paper will show that this enhanced luminescence approach easily identifies delaminated regions of plasma-sprayed TBCs. Furthermore, a case will be made that the same strong volume scattering that makes optical probing of plasma-sprayed TBCs so challenging actually enhances the contrast in luminescence intensity between attached and delaminated regions and can therefore be applied to thicker plasma-sprayed TBCs.

2. Experimental Procedures

2.1 Specimen Preparation

Freestanding TBCs were prepared as the starting point for a coating design selected to mimic defined regions of adherent and completely delaminated coating. In this demonstration coating design, the luminescent sublayer was deposited separately on the backside of the freestanding TBC and a metallic coating was deposited over well defined sections of the TBC backside to mimic an attached substrate. The freestanding TBCs of various thicknesses were produced by atmospheric plasma-spraying 8 wt% yttria-stabilized zirconia (8YSZ) powder (Zircoa, Inc., Solon, OH) onto sacrificial carbon disks (25.4 mm diameter x 3.2 mm thick) and then burning off the carbon at 800°C in air. The luminescent sublayer was then deposited onto the backside of the freestanding 8YSZ coatings by EB-PVD. YSZ itself can be an effective host matrix for rare earth dopants to produce luminescence, [8-9] so rare earth dopants for YSZ were selected that exhibit significant luminescence excitation peaks at visible wavelengths that can penetrate through plasma-sprayed 8YSZ, since 8YSZ is opaque to the ultraviolet excitation wavelengths that are conventionally used to produce luminescence.[10] YSZ doped with europium (YSZ:Eu) and YSZ doped with erbium (YSZ:Er), with excitation peaks at 535 and 517 nm, respectively, were selected for the luminescent sublayers. The pellets used as the luminescent layer source material

were hot pressed (Plasmaterials, Livermore, CA) from doped YSZ:Eu (mol% composition $88ZrO_2$-$9YO_{1.5}$-$3EuO_{1.5}$) and YSZ:Er (mol% composition $88ZrO_2$-$9YO_{1.5}$-$3ErO_{1.5}$) powder (Phosphor Technology Ltd, Norton Park, UK). Half of the backside of each freestanding 8YSZ coating was masked, and a 25-μm-thick luminescent sublayer was deposited by EB-PVD on the remaining unmasked half. To mimic an adherent substrate, a 5-μm-thick NiCr (70wt% Ni – 30 wt% Cr) layer was subsequently sputter-deposited over the freestanding coatings positioned with the luminescent layer on top and masked in a direction perpendicular to the masking performed for the luminescent sublayer deposition. The resultant partitioned multilayer freestanding coating, with the undoped plasma-sprayed 8YSZ on top, was comprised of four well defined quadrants (Fig. 1), where quadrant 1 consists of undoped plasma-sprayed 8YSZ above either a YSZ:Eu or YSZ:Er luminescent sublayer; quadrant 2 consists of the undoped 8YSZ above the luminescent layer backed by the NiCr layer; quadrant 3 consists of the undoped 8YSZ directly backed by the NiCr layer (no luminescent sublayer); and quadrant 4 consists of only the undoped 8YSZ coating. Therefore, the luminescence intensity contrast between quadrants 1 and 2 should mimic the contrast between a detached and adherent TBC and quadrant 4 will represent the background luminescence from any Eu or Er impurities in the undoped 8YSZ coating. All images will be displayed with the same quadrant orientation illustrated in Fig. 1.

2.2 Luminescence Measurements

Luminescence intensity mapping of the specimens was performed with a Renishaw System 2000 (New Mills, UK) microscope equipped with a Prior ProScan II automated scanning stage. The excitation source for luminescence from specimens with YSZ:Eu layers was a Nanogreen (JDS Uniphase, San Diego, CA) pulsed frequency-doubled 532 nm (overlapping the YSZ:Eu 535 nm excitation) YAG:Nd laser operating at a power of 4 μJ/pulse and a frequency of 5.3 kHz. The

excitation source for luminescence from specimens with YSZ:Er layers was a Spectra-Physics (Mountain View, CA) continuous argon ion 514 nm (overlapping the YSZ:Er 517 nm excitation) laser operating at a power of 25 mW. For both cases, the laser excitation was transmitted through a 20x objective and defocused to a diameter of 100 μm before striking the specimen placed on the automated scanning stage. A scanning luminescence intensity map was generated by stepping (step size = 400 μm) the specimen position beneath the microscope objective in a raster pattern to cover a 28 mm x 28 mm area containing the 25.4 mm diameter specimen. After each step, a luminescence emission spectrum was collected (3 sec acquisition time), and the luminescence intensity was calculated from the area under the emission peak after baseline subtraction. In this manner, a 71x71 pixel image was generated with each pixel representing the luminescence intensity measured at that location.

To demonstrate an implementation of luminescence intensity mapping that is more practical than the scanning luminescence mapping (acquisition time over 8 hr for each specimen), luminescence intensity imaging with acquisition times of 10 sec was performed without spectral acquisition. Luminescence images of the specimens with YSZ:Eu luminescent sublayers were collected using a 200mW 532 nm CW laser diode (Intelite, Genoa, NV) coupled to a 100μm graded indexed fiber producing a uniform spot. The laser light is projected through a pair of cylindrical lenses on a scanned mirror that focuses the beam shape to a line with a width of 0.5mm and a length of 35 mm. The mirror was scanned with a triangular waveform input at 100Hz to provide uniform excitation over the entire sample surface. Direct imaging of luminescence emission intensity at 606 nm was performed using a bandpass filter centered at 610 nm with a bandwidth (FWHM) of 10 nm along with a 590 nm longpass filter coupled through a 105 mm Nikkor lens fitted to a cooled slow-scan camera (Photometrics Series 300).

3. Results

Luminescence emission spectra from quadrants 1, 2, and 4 (as designated in Fig. 1) of a 123-μm-thick plasma-sprayed 8YSZ freestanding specimen with backside YSZ:Eu and NiCr coatings are shown in Fig. 2. Because the 606 nm emission intensity from quadrants 2 and 4 is much lower than from quadrant 1, the spectra from quadrants 2 and 4 were multiplied by a factor of 10 for easier comparison. Fig. 2 shows that the addition of a backside NiCr layer below the YSZ:Eu layer (quadrant 2) results in a dramatic decrease, by a factor of about 20, in the 606 nm emission intensity observed without the NiCr layer (quadrant 1). Because the contrast between these two quadrants is similar to what would be expected between a detached and an adherent TBC with the same YSZ:Eu base layer, this very large luminescence intensity "enhancement" from regions without a metallic backing provides excellent discrimination for identifying regions of TBC delamination. The emission spectrum from quadrant 4 (Fig. 2), where there is no YSZ:Eu or NiCr underlayer, reveals a small but significant emission peak that can be attributed to trace Eu impurities in the undoped 8YSZ.

To investigate the potential applicability of using luminescence intensity measurements to identify delaminated regions over a range of plasma-sprayed TBC thicknesses, scanning luminescence intensity maps (606 nm emission) were collected from 123, 215, and 302 μm thick plasma-sprayed 8YSZ freestanding specimens with backside YSZ:Eu and NiCr coatings. Fig. 3 displays the luminescence intensity maps for each thickness with dashed lines added to indicate the delineation between the quadrants. Consistent with the emission intensities observed in Fig. 2, the presence or absence of the NiCr backing beneath the YSZ:Eu layer produces significant

contrast. In each case, quadrant 1, where the YSZ:Eu sublayer has no NiCr backing, is much brighter than quadrant 2, where the YSZ:Eu sublayer does have a NiCr backing. It is quite striking that the luminescence intensity observed from the YSZ:Eu layer is reduced so severely by the presence of the NiCr backing that when displayed on a linear scale that is wide enough for quadrant 1 not to reach saturation levels, there is no discernible contrast between quadrant 2, with the NiCr-backed YSZ:Eu sublayer, and quadrants 3 and 4, which have no YSZ:Eu sublayer. The luminescence intensity from quadrant 1, which mimics a delaminated region, is attenuated about an order of magnitude for each ~100 μm increment in 8YSZ thickness (comparing Figs. 3a, 3b, and 3c); however, the contrast associated with the NiCr backing is not seriously degraded until the intensity of the luminescence observed from the Eu impurities in the plasma-sprayed 8YSZ coating (quadrant 4) becomes a significant fraction of the intensity of the luminescence observed from the YSZ:Eu sublayer (quadrant 1) as seen in Fig. 3c for the 302-μm-thick 8YSZ specimen. Therefore, the thickness limitation for observing contrast between unbacked and NiCr-backed YSZ:Eu sublayers depends on the Eu impurity level in the undoped plasma-sprayed 8YSZ, which produces a background luminescence intensity level that cannot be distinguished from the luminescence originating from the YSZ:Eu sublayer.

To demonstrate that diagnostically effective luminescence contrast can be obtained with acquisition times that are sufficiently short for practical inspection, Fig. 4 shows a luminescence intensity map that was collected by simple emission bandpass imaging for the 123-μm-thick plasma-sprayed 8YSZ freestanding specimen with backside YSZ:Eu and NiCr coatings. The acquisition time for the luminescence intensity map obtained by simple emission bandpass imaging (Fig. 4) was only 10 sec, compared to over 8 hr acquisition time for the luminescence intensity map of the same specimen collected by scanning spectral intensity mapping (Fig. 3a). In

Fig. 4, the original image intensity has been normalized to the area-averaged intensity over quadrant 2, where the YSZ:Eu underlayer is NiCr-backed. Therefore, the average normalized intensity is unity in quadrant 2, and the normalized intensity in quadrant 1 represents the luminescence intensity enhancement factor associated with the removal of the metallic backing. Fig. 5 displays a line scan (lower curve) corresponding to the dashed line marker in Fig. 4, passing upwards from quadrant 2 to quadrant 1, and shows that the absence of the metallic backing increases the luminescence intensity by about a factor of four for the simple emission bandpass image. Also plotted in Fig. 5 is an identically located line scan from a similarly normalized scanning spectral intensity map of the same specimen (Fig. 3a), which reveals an average luminescence intensity enhancement of about 20-fold. The lower luminescence intensity enhancement, and therefore lower contrast, in the luminescence intensity map obtained by simple emission bandpass imaging is most likely a consequence of the background subtraction that is incorporated into the scanning spectral intensity map, but not into the simple emission-bandpass-filter-based image. While using a bandpass filter (instead of spectral acquisition) reduced the luminescence intensity enhancement factor associated with the absence of a metallic backing (from about 20 to 4), the enhancement is still easily observed (Fig. 4), and the tremendous reduction in acquisition time (from hours to seconds) makes the simple emission bandpass imaging approach much more suitable for practical application. Additionally, the lateral resolution is superior using the imaging approach (Fig. 4) compared to the step-size-controlled resolution of the scanning spectral intensity maps (Fig. 3b).

Because of its strong excitation peak in the visible wavelength range at 517 nm, YSZ:Er was also considered as a promising candidate for producing reflectance-enhanced luminescence for indicating TBC delamination. Specimens were prepared with the same configuration shown in Fig. 1 except that the 25-μm-thick YSZ:Eu layer was replaced with a YSZ:Er layer of the same

thickness. Fig. 6 shows a luminescence emission spectrum from the YSZ:Er layer above a 127-μm-thick plasma-sprayed 8YSZ layer, indicating strong emission at 562 nm. Also shown, both multiplied by a factor of 10, are emission spectra for the same YSZ:Er layer below the undoped YSZ layer (quadrant 1) as well as from quadrant 4, where there is no YSZ:Er layer. Unfortunately, there was no significant difference in the luminescence intensity observed from the unbacked YSZ:Er underlayer and the luminescence intensity originating solely from Er impurities in the plasma-sprayed 8YSZ layer. The strong background 562 nm luminescence from the Er impurities in the plasma-sprayed 8YSZ layer thus masks observation of luminescence from the YSZ:Eu underlayer, even when the overlying undoped 8YSZ layer is only 127 μm thick.. The Er impurity concentration in the undoped plasma-sprayed 8YSZ was 80 ppm by weight, measured by inductively coupled plasma spectrometry, clearly indicating that a very minor concentration of Er was responsible for the interfering luminescence background.

4. Discussion

The much stronger luminescence intensity observed from the unbacked YSZ:Eu underlayer compared to the NiCr-backed YSZ:Eu underlayer (Figs. 2-4) indicates that the reflectance-enhanced luminescence can be used to monitor TBC delamination progression even in highly scattering plasma-sprayed TBCs, since delaminated regions of TBCs should show similar reflectance-enhanced luminescence. Fast capture (seconds) of luminescence intensity images by simple imaging through an emission bandpass filter provides more than sufficient contrast to identify regions of TBC delamination (Fig. 4). The successful application of reflectance-enhanced luminescence to highly scattering plasma-sprayed TBCs relies on the scattering actually increasing contrast, as opposed to degrading contrast as observed with other techniques. Scattering has a large effect because plasma-sprayed TBCs are so strongly scattering that virtually no light is transmitted a significant distance through the TBC unscattered. [11]

Therefore, luminescence emission originating in the YSZ:Eu layer at the bottom of the coating most likely must experience multiple reflections at the coating back surface before it can escape out the front surface to be observed. Multiple reflections of luminescence emission at the coating back surface increases contrast because of the higher survival rate of light reflecting against the back of a delaminated TBC versus reflecting against the back of a TBC attached to its metal substrate. The reflectivity at the TBC/air gap interface at the back of a delaminated (unbacked) TBC is very high because a large fraction of the incident light has an angle of incidence above the critical angle for total internal reflection due to the large difference in index of refraction, n, between the TBC (n = 2.2 at 500 nm wavelength for 8YSZ) and air (n = 1.0). This difference in index of refraction can be used to predict [7] the diffuse reflectivity at the back side of the delaminated TBC, $\rho_{delaminated} = 0.83$. Hemispherical reflectance measurements of a bare NiCrAlY bond coat were used to estimate the reflectivity at the back surface of an attached TBC, $\rho_{attached} = 0.35$. Making the simplifying assumption that any light transmitted through the back of the delaminated TBC is eventually absorbed, the survival rate for luminescence after multiple reflections from the back of the TBC is ρ^N, where N is the number of multiple reflections. The attached to delaminated luminescence survival ratio for multiple backside reflections is therefore $(\rho_{attached}/\rho_{delaminated})^N$ and decrease rapidly from 0.42 to 0.18 to 0.07 for N = 1, 2, and 3, respectively. This shows that just a few backside reflections, caused by TBC internal scattering, will greatly accentuate the contrast between regions of attached and delaminated TBC. This improved contrast arises just because the luminescence attenuation is much greater for the attached TBC. However, there is a thickness limit to exploiting this accentuated contrast, because the background luminescence intensity level eventually becomes a significant fraction of the attenuated luminescence transmitted through the undoped TBC, thereby degrading contrast. In particular, trace impurities in the overlying undoped TBC of the same rare earth dopant present in

the luminescent sublayer will produce luminescence that cannot be distinguished from luminescence originating from the luminescent sublayer. With increasing TBC overlayer thickness, the luminescence observed from the luminescent sublayer will become so attenuated that it will be overwhelmed by luminescence from the rare earth impurities within the undoped TBC overlayer, as observed for the YSZ:Er layer, where there was no contrast between an unbacked and a NiCr-backed YSZ:Er underlayer below a 127-μm-thick undoped 8YSZ layer.

A major challenge for adapting reflectance-enhanced luminescence for monitoring delamination in plasma-sprayed TBCs is to seamlessly integrate the luminescent sublayer into the plasma-sprayed TBC. In the investigation described here, the YSZ:Eu and YSZ:Er luminescent sublayers were deposited by a EB-PVD, producing a denser microstructure than the plasma-sprayed 8YSZ overlayer. Undoubtedly, adding a microstructurally distinct luminescent sublayer next to the bond coat will adversely affect the TBC lifetime. Therefore, future efforts should be directed towards integrating the luminescent sublayer into the plasma-spray deposition process.

5. Summary

To test the use of luminescence intensity measurements as an indication of TBC delamination, a freestanding coating design was implemented that incorporated a luminescent sublayer and contained well delineated areas that served as models for an attached or delaminated TBC in order. For specimens with a YSZ:Eu luminescent sublayer, “delaminated” sections, i.e.,with no NiCr backing, exhibited a much higher luminescence intensity than “attached” sections, i.e., with NiCr backing, and contrast between these regions remained quite evident even at a plasma-sprayed 8YSZ overlayer thickness of 300 μm. The contrast between “delaminated” and “attached” regions is created by the reflectance-enhanced luminescence from the “delaminated” section and is due to the significantly higher reflectivity at the coating/air gap interface as

compared to the coating/NiCr interface. The application of reflectance-enhanced luminescence is particularly well suited to plasma-sprayed TBCs because their highly scattering nature, instead of degrading contrast, actually increases the contrast in luminescence intensity between delaminated and attached regions. It is proposed that internal TBC scattering favors multiple reflections of luminescence emission from the bottom surface of the TBC before luminescence can escape through the top surface of the TBC. The contrast between delaminated and attached regions will be accentuated by multiple reflections because of the higher survival rate of light reflecting off the back surface of a delaminated TBC, as opposed to an attached TBC. Background luminescence, particularly from luminescent impurities in the undoped TBC layer, degrades contrast between delaminated and attached regions for thicker TBCs. Background luminescence can be a problem even at low impurity concentrations, as observed for YSZ:Er layers, where luminescence from Er impurities in the undoped YSZ layer overwhelmed luminescence observed from the YSZ:Er sublayer.

References

1. D. Zhu and R.A. Miller, MRS Bull., 25 (2000) 43-47.

2. J.T. DeMasi-Marcin, K.D. Sheffler, and S. Bose, ASME J. Eng. Gas Turbines and Power, 112 (1990) 521-526.

3. X. Peng and D.R. Clarke, J. Am Ceram. Soc., 83 (2000) 1165-1170.

4. W.A. Ellingson, R.J. Visher, R.S. Lipanovich, and C.M. Spuckler, Mater. Eval., 64 (2006) 45.

5. M. Gell, S. Sridharan, M. Wen, and E.H. Jordan, Int. J. Appl. Ceram. Technol., 1 (2004) 316-329.

6. J. I. Eldridge, C.M. Spuckler, J.A. Nesbitt, and R.E. Martin, Ceram. Eng. Sci. Proc., 26 (2005) 121-128.

7. J. I. Eldridge, C.M. Spuckler, and R.E. Martin, Int. J. Appl. Ceram. Technol., 3 (2006) 94-104.

8. J.P. Feist and A.L. Heyes, “Development of the Phosphor Thermometry Technique for Application in Gas Turbines,” 10th Int. Symp. On Applications of Laser Techniques to Fluid Mechanics, Lisbon, Portugal, 2000.

9. M.M. Gentleman and D.R. Clarke, Surf. Coat. Technol., 188-189, (2004) 93-100.

10. J.I. Eldridge, T.J. Bencic, S.W. Allison, and D.L. Beshears, J. Thermal Spray Technol., 13 (2004) 44-50.

11. J.I. Eldridge, C.M. Spuckler, K.W. Street, and J.R. Markham, Ceram. Eng. Sci. Proc., 23 (2002) 417-430.

Figure Captions

Fig. 1. Diagram of the coating design divided into quadrants as viewed from above. Quadrant 1 consists of undoped YSZ layer above YSZ:Eu (or YSZ:Er) luminescent sublayer. In quadrant 2, luminescent sublayer is backed by NiCr coating. Quadrant 3 consists of undoped YSZ layer directly above NiCr coating (no luminescent sublayer). Quadrant 4 consists of only undoped YSZ layer.

Fig. 2. Comparison of 606 nm emission spectra from (1) unbacked YSZ:Eu sublayer below 123-μm thick undoped plasma-sprayed 8YSZ (quadrant 1), (2) NiCr-backed YSZ:Eu sublayer below same undoped 8YSZ (quadrant 2), and (3) undoped 8YSZ alone (quadrant 4). Spectra from quadrants 2 and 4 have been multiplied by a factor of 10.

Fig. 3. Scanning luminescence spectral intensity maps showing reflectance-enhanced luminescence from unbacked YSZ:Eu layer (quadrant 1) below range of plasma-sprayed 8YSZ thicknesses. Plasma-spray 8YSZ thicknesses are (a) 123 μm, (b) 215 μm, and (c) 302 μm.

Fig. 4. Luminescence intensity image collected by imaging through emission bandpass filter of same specimen as shown in Fig. 3a. Acquisition time was 10 sec.

Fig. 5. Intensity line scan (lower curve) from normalized luminescence intensity image displayed in Fig. 4. Location of line scan indicated by dashed line in Fig. 4; direction of scan is upward from quadrant 2 to quadrant 1.Upper curve is the identically located line scan from scanning spectral intensity map (Fig. 3b) after similar normalization to quadrant 2.

Fig. 6. Comparison of 562 nm emission spectra from (1) YSZ:Er sublayer above 127-μm-thick undoped plasma-sprayed 8YSZ, (2) same YSZ:Er sublayer below same undoped plasma-sprayed 8YSZ (quadrant 1), and (3) undoped plasma-sprayed 8YSZ alone (quadrant 4). Lower two spectra (quadrants 1 and 4) have been multiplied by a factor of 10.

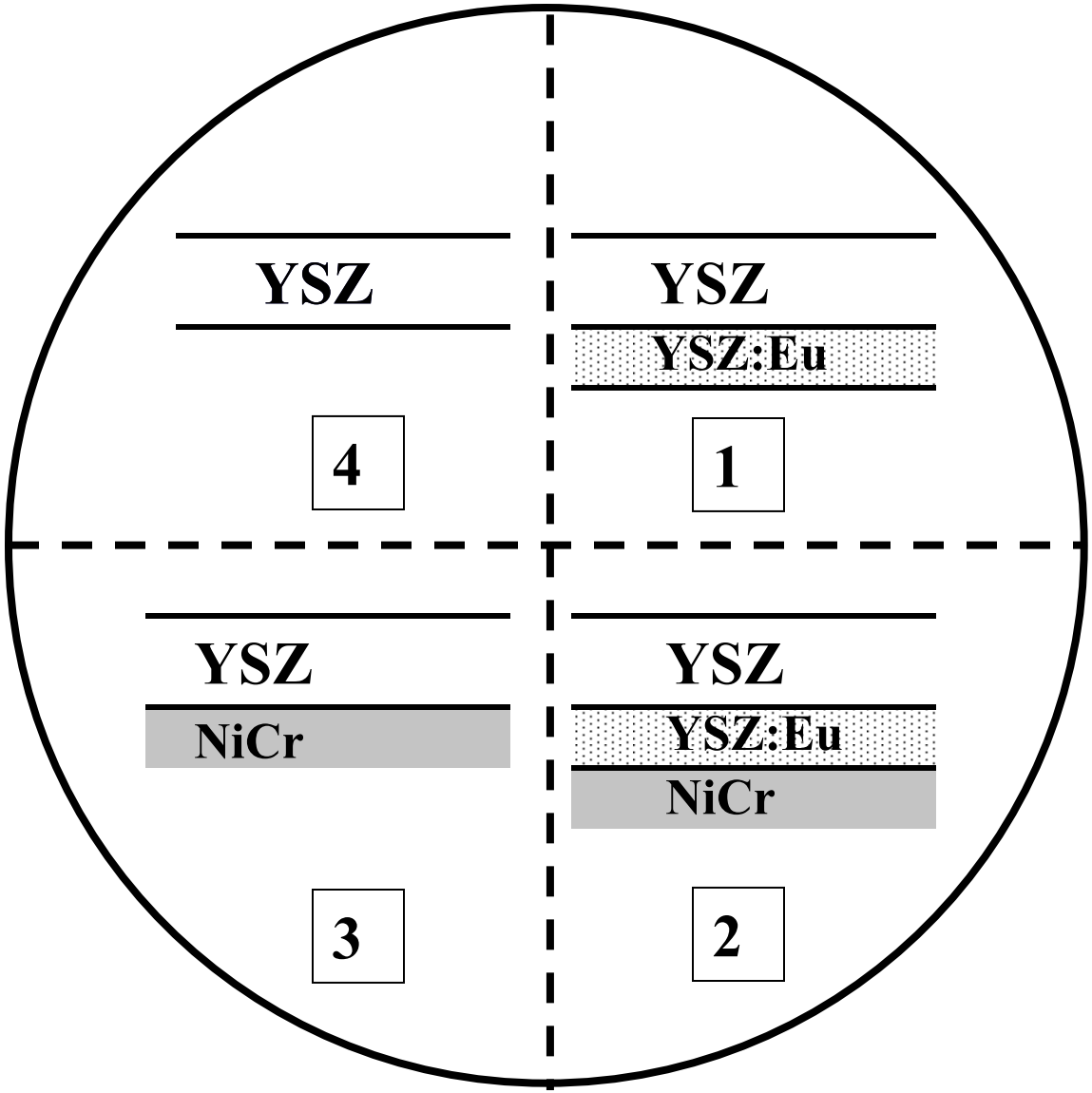

Fig. 1

Fig. 2

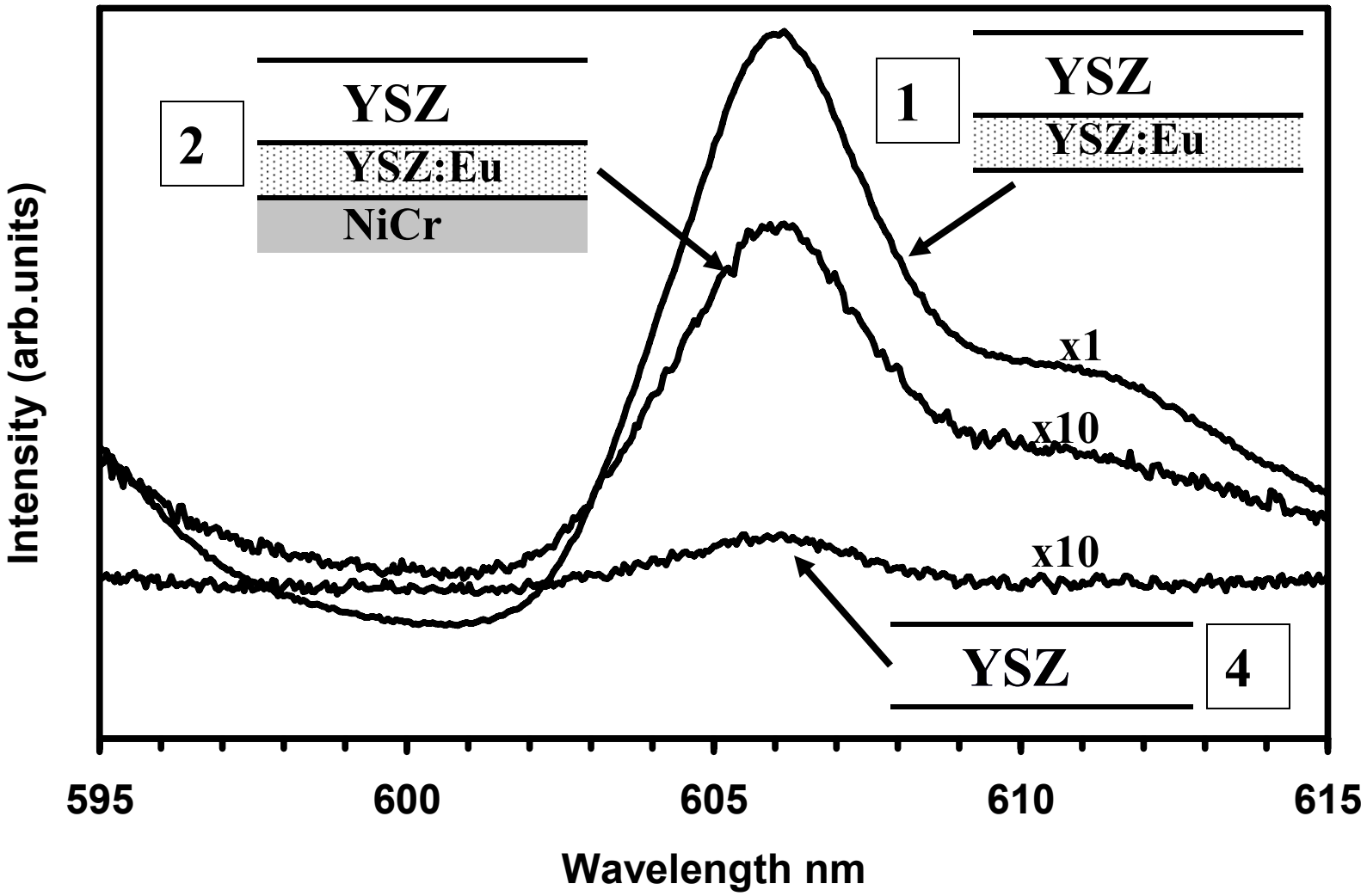
Intensity (arb.units)
595
600
605
610
615
Wavelength nm
2
YSZ
YSZ:Eu
NiCr
1
YSZ
YSZ:Eu
x1
x10
x10
YSZ
4

Fig. 3

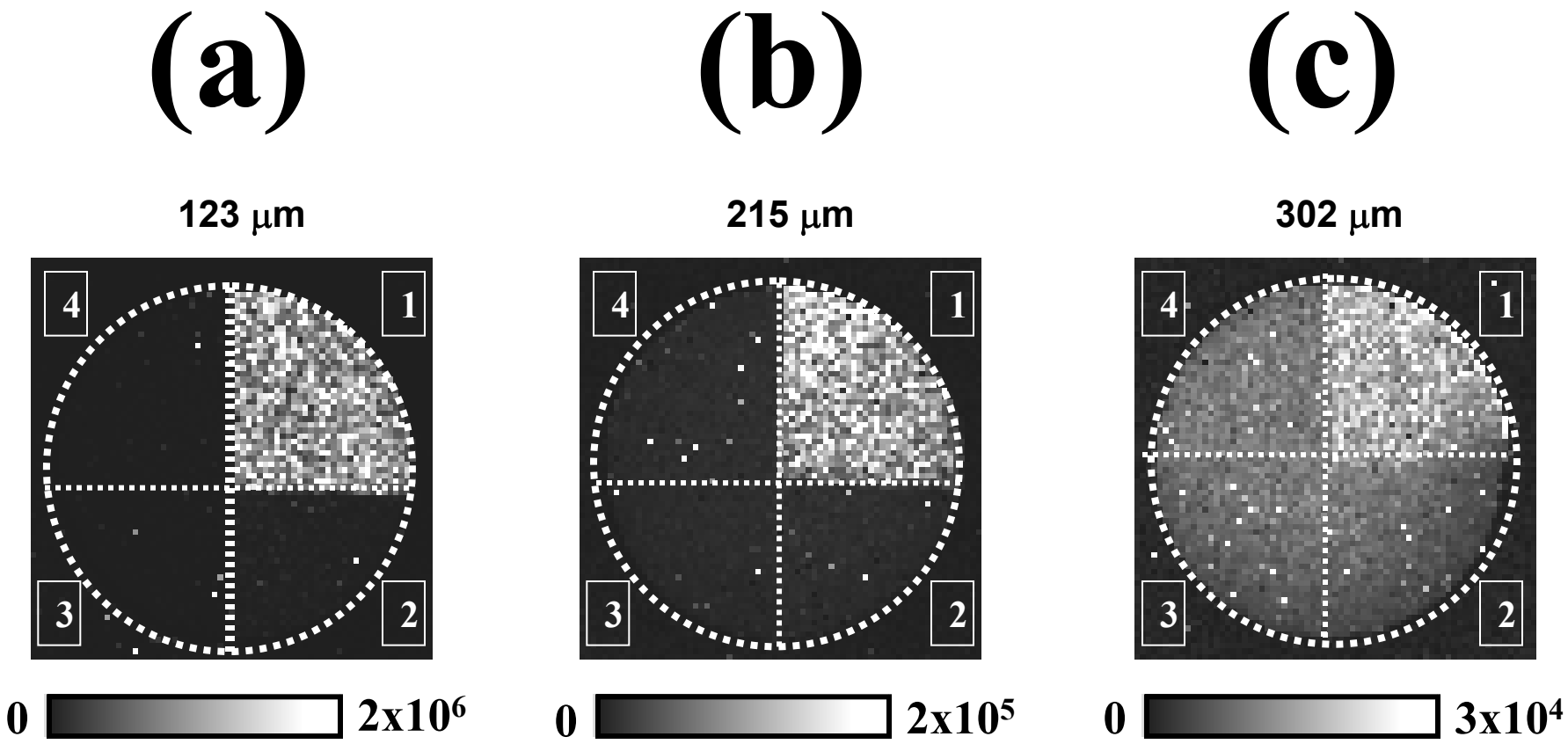

Fig. 4

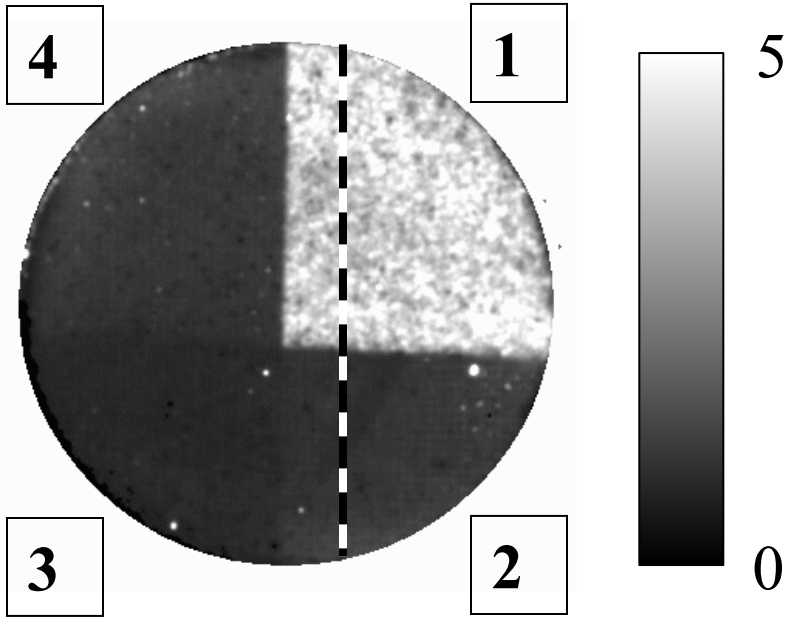

Fig. 5

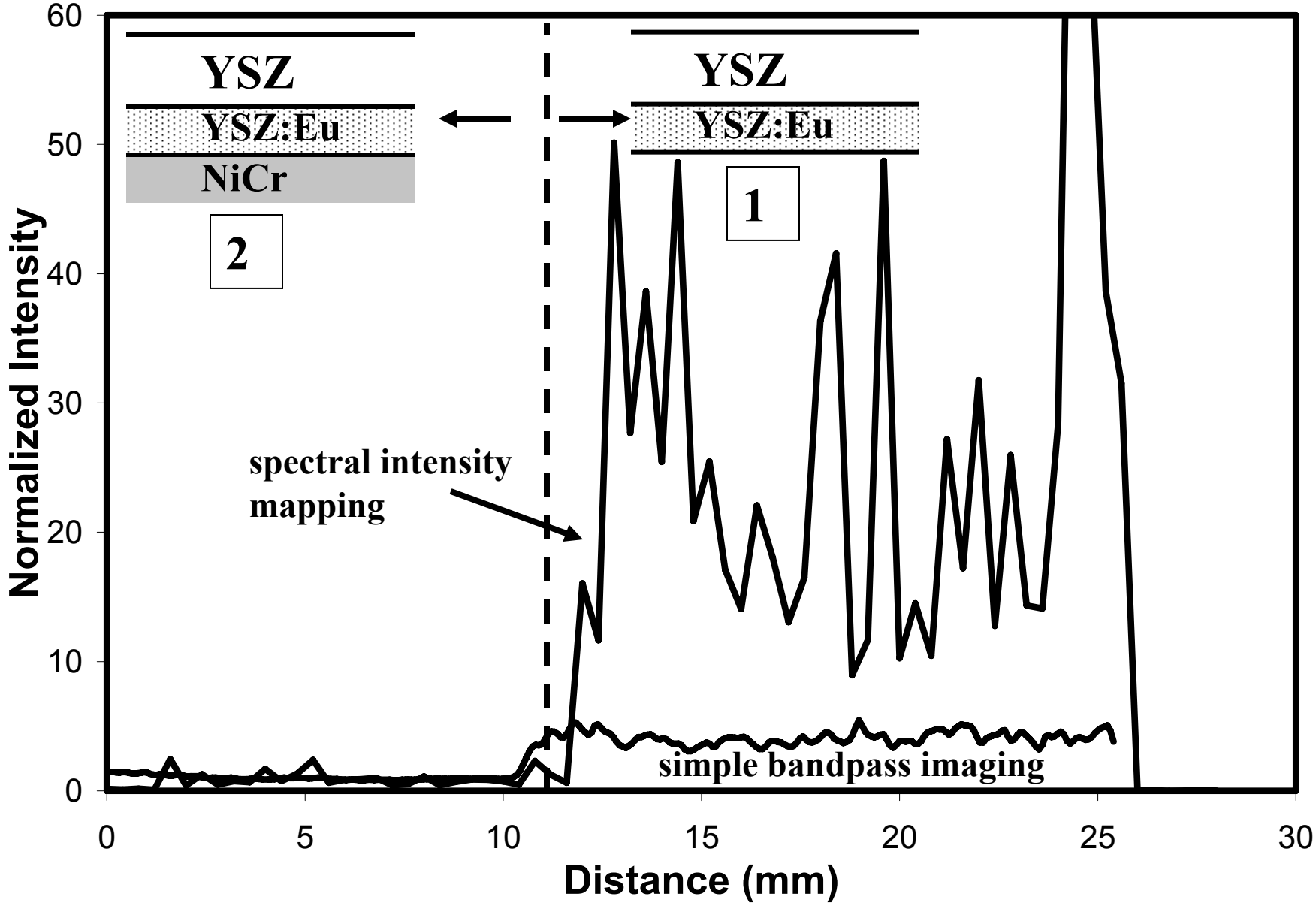
YSZ
YSZ:Eu
NiCr
2
YSZ
YSZ:Eu
1
spectral intensity mapping
simple bandpass imaging
Normalized Intensity
Distance (mm)
0
10
20
30
40
50
60
0
5
10
15
20
25
30

Fig. 6

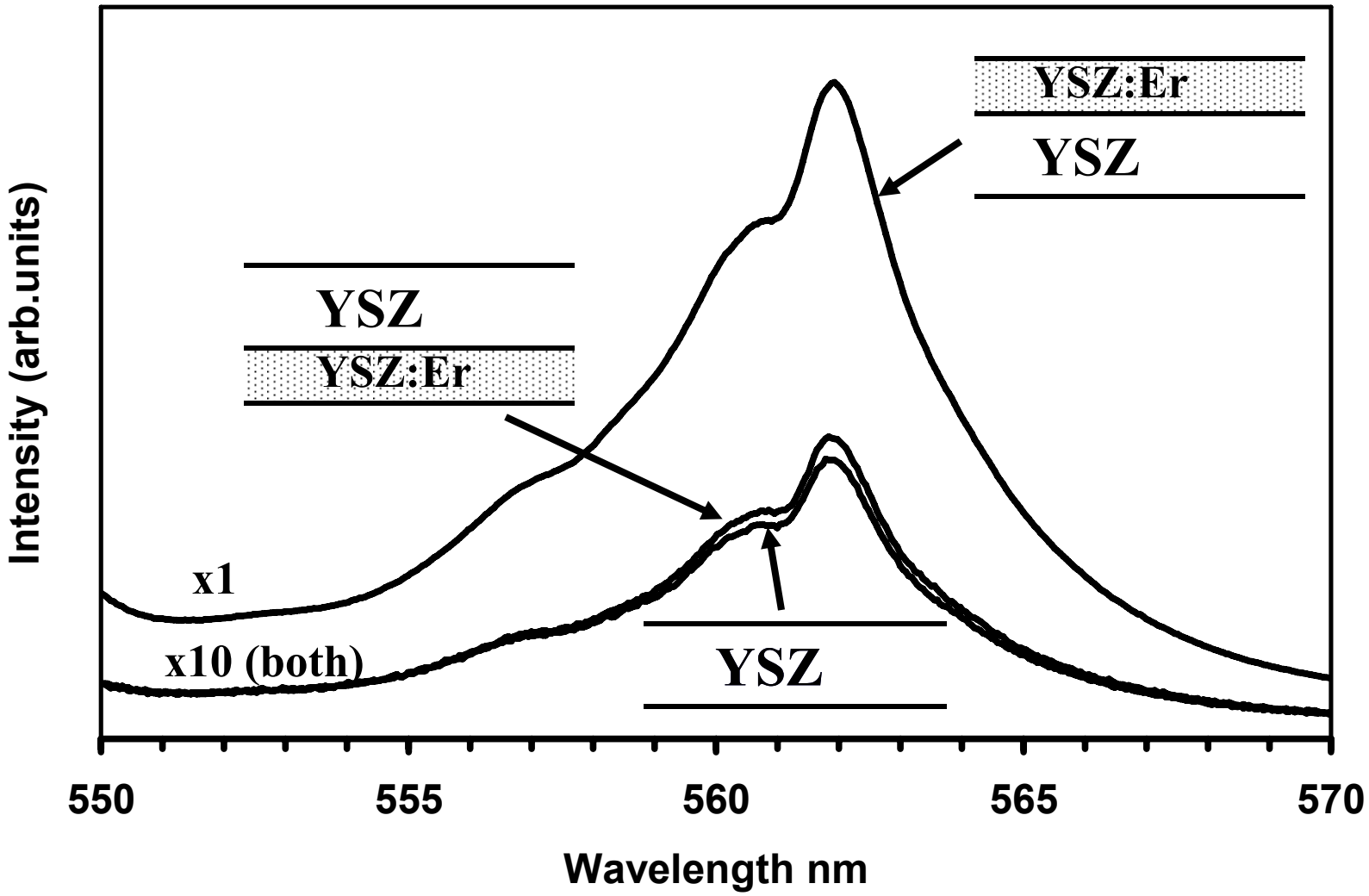
YSZ:Er
YSZ
YSZ
YSZ:Er
x1
x10 (both)
YSZ
Intensity (arb.units)
550
555
560
565
570
Wavelength nm